The accuracy of TIP4P/2005 and SPC/Fw water models

João V. L. Valle,[†] Bruno H. S. Mendonça,[‡] Marcia C. Barbosa,[¶] Helio Chacham,[§] and Elizane E. de Moraes[*,†]

[†]*Instituto de Física, Universidade Federal da Bahia, Campus Universitário de Ondina, Salvador 40210-340, BA, Brazil*

[‡]*Departamento de Física, ICEX, Universidade Federal de Minas Gerais, CP 702, Belo Horizonte 30123-970, MG, Brazil*

[¶]*Instituto de Física, Universidade Federal do Rio Grande do Sul, Porto Alegre 91501-970, RS, Brazil*

[§]*Departamento de Física, ICEX, Universidade Federal de Minas Gerais, CP 702, 30123-970 Belo Horizonte, Minas Gerais, Brazil*

E-mail: elizane.fisica@gmail.com

Abstract

Water is used as a main solvent in model systems containing bioorganic molecules. Choosing the right water model is an important step in the study of biophysical and biochemical processes that occur in cells. In the present work, we perform molecular dynamics simulations using two distinct force fields for water - the rigid model TIP4P/2005, where only intermolecular interactions are considered, and the flexible model SPC/Fw, where intramolecular interactions are also taken into account. The simulations aim to determine the effect of the inclusion of intramolecular interactions on the accuracy of calculated properties of bulk water (density and thermal expansion

coefficient, self-diffusion coefficients, shear viscosity, radial distribution functions, and dielectric constant), as compared to experimental results, over a temperature range between 250 K and 370 K. We find that the results of the rigid model present the smallest deviations relative to experiments for most of the calculated quantities, except for the shear viscosity of supercooled water and the water dielectric constant, where the flexible model presents better agreement with experiments.

Introduction

Water is abundant in liquid solid forms in our planet, and it exhibits several thermodynamic, dynamic and structural anomalous behaviors.[1–13] From agriculture to travel, public health to commerce, water's properties shape human activity and define the geography, topography, and environment in which we live.[14,14–25] Water is so central to life on Earth that it conditions the search for the possibility of life elsewhere.[15] Many living beings can survive only a few days without water because it is involved in most biological processes,[16] such as nutrient metabolism catalyzed by enzymes, and it serves as a medium for cell communication.

Although water molecules have simple geometric structures, this molecular liquid is still challenging for experimental, theoretical, and computational methods. Water is a complex substance to model, because of the competing effects of hydrogen bonding and van der Waals interactions. In the past few decades, much effort from the molecular dynamics (MD) simulation community has been devoted to develop force field models to simulate bulk and confined water. These include models with three, four, and five, coulomb interaction sites with rigid or flexible geometry, and other models that incorporate the electronic polarization.[26–49] Recently, new models have also been parameterized from a deep neural network.[36,39] In general, each of these water models has been optimized to reproduce only a few of the thermodynamic properties of water, usually from experimental data. In this context, their success depends on being able to reproduce additional experimental properties both in bulk and confined water. A force field capable of describing the macroscopic properties of bulk and

confinement systems at the same time is still a significant challenge. The challenge is to define the minimum and simplest model which is able to describe distinct anomalous and non-anomalous thermodynamic, dynamic, and structural properties of water.

TIP4P/2005 is one of the most used rigid models.[28] It is composed of four points: oxygen with mass, two hydrogen with positive charges, and a fictitious location between the oxygen and hydrogen to represent the dislocated charge of oxygen. This model was parameterized using experimental data such as the maximum density temperature, the enthalpy of vaporization, and the density of liquid water at ambient conditions. It can reproduce thermodynamic and dynamic properties of water in a wide range of temperatures[28] but is not able to capture the changes in the water polarization due to variations in temperature and pressure. To circumvent this limitation, flexible models were created. They represent the O-H bond lengths and angles by harmonic functions and are better equipped to reproduce flexibility transport properties.[27] Even though these models provide good agreement with experiments for phase coexistence, dielectric constants, viscosity, and diffusion,[50] they do not significantly improve the prediction of thermodynamic properties in general.[51,52]

Anders Wallqvist and Olle Teleman[53] indicated that the reason for the better description of the water dynamics by flexible models when compared with rigid models is that the flexibility slows down the motion of isolated water molecules, probably due to the increase of the dipole moment. Then, while thermodynamic properties would be more dependent on the local arrangements if water forms open or close clusters, the dynamics would be the result of a more global organization. This suggests that what defines if the water property can be described by a rigid or a flexible model is whether it depends on the local structure being short range or if it is dependent on the dipole-type longer range interaction. For instance, density, specific heat, and compressibility are usually well represented by rigid models since they are properties that depend on the two-length scales interactions, tetrameters connected by hydrogen bonds, or by van der Waals interactions. These "volumetric" properties can even be represented by effective potentials[54] which take into account the competition between

these length scales, but which do not exhibit any long-range interaction.

Among the several flexible models, the SPC/Fw[55] and SPC/FH[35] models are the simplest systems. They were fitted from the three points SPC to describe dynamic properties even for the system under confinement[52,56] On the other hand, TIP4P/2005[57,58] and TIP4P/ϵ[59] give an outstanding agreement with the experimental results for a wide range of properties. This raises the question of what flexibility does actually add to the description of the system properties.

In this work, we attempt to answer the question of the role of flexibility by evaluating the dynamic, transport, and thermodynamic properties of bulk water for the models TIP4P/2005 and SPC/Fw. The properties will be separated in to two types: "volumetric" and "electrostatic". The first group refers to water anomalies that appear event in effective models where the electrostatic effects are not present directly. The second group is related to the effects that are of long-range interaction and where water dipole might play a relevant role.

The remainder of this paper goes as follows. In Sec. II computational details are presented. Results are discussed in Sec. III, while conclusions are shown in Sec. IV.

Methods

We performed molecular dynamics simulations in the canonical NVT or isothermal-isobaric NPT ensembles at 1 bar and a range of temperatures, using the LAMMPS package.[60] The simulation box was filled with 512 molecules and periodic boundary conditions (PBC) were applied in all directions. The Nosé-Hoover chains of thermostat and barostat were employed to keep temperature and pressure constant. The equations of motion were solved using the Nosé-Hoover integration scheme with a timestep of 1 fs for the rigid model and 0.5 fs for the flexible models. This choice of timestep is compatible with the literature.[61] The equilibration runs lasted between 3 ns and 10 ns, whilst the production was longer than 15 ns.

For water, we used the rigid model TIP4P/2005[28] which reproduces several thermodynamic water properties conditions[57,58] and the flexible SPC/Fw[55] model which reproduce water dynamic properties. The models use Lennard-Jones and Coulomb potentials to describe the intermolecular interactions,

$$U_{ij} = 4\epsilon \left[\left(\frac{\sigma}{r_{ij}} \right)^{12} - \left(\frac{\sigma}{r_{ij}} \right)^{6} \right] + \frac{1}{4\pi\epsilon_o} \frac{q_i q_j}{r_{ij}} \tag{1}$$

where r_{ij} is the distance between sites i and j, q_i is the electric charge of a site i, ϵ_o is the permittivity of vacuum, ϵ is the LJ energy scale and σ is the repulsive diameter for a pair ij. For the flexible models, an additional term is included to account for the intramolecular interactions that are defined, in the present work, by harmonic potentials in bonds and angles,

$$U(r) = \frac{k_{OH}}{2}(r - r_o)^2 \tag{2}$$

and

$$U(\theta) = \frac{k_\theta}{2}(\theta - \theta_o)^2 \tag{3}$$

where k is the corresponding spring constant, r_o and θ_o are, respectively, the bond and angle at their equilibrium values. The hydrogen bonding, these interactions arise from the interplay between the oxygen and hydrogen atoms of one molecule and their corresponding atoms in neighboring molecules. These interactions are characterized by both electrostatic and Lennard-Jones (LJ) components. The electrostatic component reflects the attraction between the opposite charges of the involved atoms, while the LJ component addresses short-range repulsion and attraction contributions. The precise definition of a hydrogen bond is based on criteria related to the distance and angle between the involved atoms, providing a rigorous approach to each force field in the literature.

For the rigid model, the intramolecular part was constrained by using the SHAKE al-

gorithm with a tolerance of 10^{-4}. The force field parameters for the models are listed in Table 1. Coulomb long-range interactions were computed with the Particle-Particle-Particle-Mesh (PPPM) method, and a tail correction was added to the LJ energy evaluation.

Table 1: Force field parameters used for each of the water models. The Lennard-Jones site is located on the oxygen atom, with parameters σ and ϵ. The charges of oxygen and hydrogen are q_O and q_H, respectively. The TIP4P/2005[28] model has four interaction sites – on the three atoms, and on a fourth site along the symmetry axis between the hydrogen and oxygen atoms, which is referred to as the M site with negative charge q_M and distance to the oxygen d_{OM}

. The distance between the oxygen and hydrogen sites is r_{OH}. The angle formed between hydrogen, oxygen and another hydrogen atom is given by θ_{HOH}. For flexible model (SPC/Fw[55] the k_{OH} and k_θ are the potential depth parameters, and OH and θ are the reference bond length and angle, respectively.

	TIP4P/2005	SPC/Fw
ϵ_{OO} (kcal mol^{-1})	0.1852	0.155
ϵ_{HH} (kcal mol^{-1})	0.0	0.0
σ_{OO} (Å)	3.1589	3.165
σ_{HH} (Å)	0.0	0.0
q_O (e)	0.0	-0.82
q_H (e)	0.5564	0.41
q_M (e)	-1.1128	*
d_{OM} (Å)	0.1546	*
r_{OH} (Å)	0.9572	1.012
θ_{HOH} (°)	104.52	113.24
k_{OH} (kcal mol^{-1} Å^{-2})	*	1059.162
k_θ (kcal mol^{-1} rad^{-2})	*	75.90

Results and discussion

In order to understand the characteristics of each force field, we evaluated two sets of properties: density and thermal expansion which we identify as the "volumetric" effects and self-diffusion coefficient, shear viscosity, and Dielectric Constant which we identify as "electrostatic" effects. In order to understand the distinction between these two sets we also compared the radial distribution function of the rigid and flexible models.

Density and Thermal Expansion Coefficient

First, we explore the "volumetric" properties. Figure 1 exhibits the dependence of the density with temperature at atmospheric pressure, where the results and experimental data were fitted to a 5^{th} order polynomial in $1/T$.[28] From that, the temperature maximum of the maximum density (T_{md}) was determined by the maximum of the fitted curves.

The flexible model shows an inverse dependence of the density with temperature, without a maximum within the considered interval (250-370 K). Additional simulations with SPC/Fw at temperatures below 250 K show that it exhibits a maximum density at 254 K. The TIP4P/2005, as expected, reproduces very well the water anomaly, showing a maximum at 277.3 K (only 0.3 K higher than the experimental value of 277 K) with a density of 1.0 g/cm^3.

The agreement between TIP4P/2005 and the experiment is excellent at all temperatures above room temperature (298-370 K), with no systematic deviation being observed in this temperature range. Note that most of the differences in relation to the experimental values are due to the degree of freedom and flexibility of the models, where for temperatures below the ambient temperature 298 K the flexible model loses effectiveness and results in a denser structure in relation to the rigid model. This fact may be related to the ability to form and break hydrogen bonds, where the flexible model favors at low temperatures a capacity to form hydrogen bonds greater than the rigid one and therefore suffer an increase in density in relation to the experimental values.

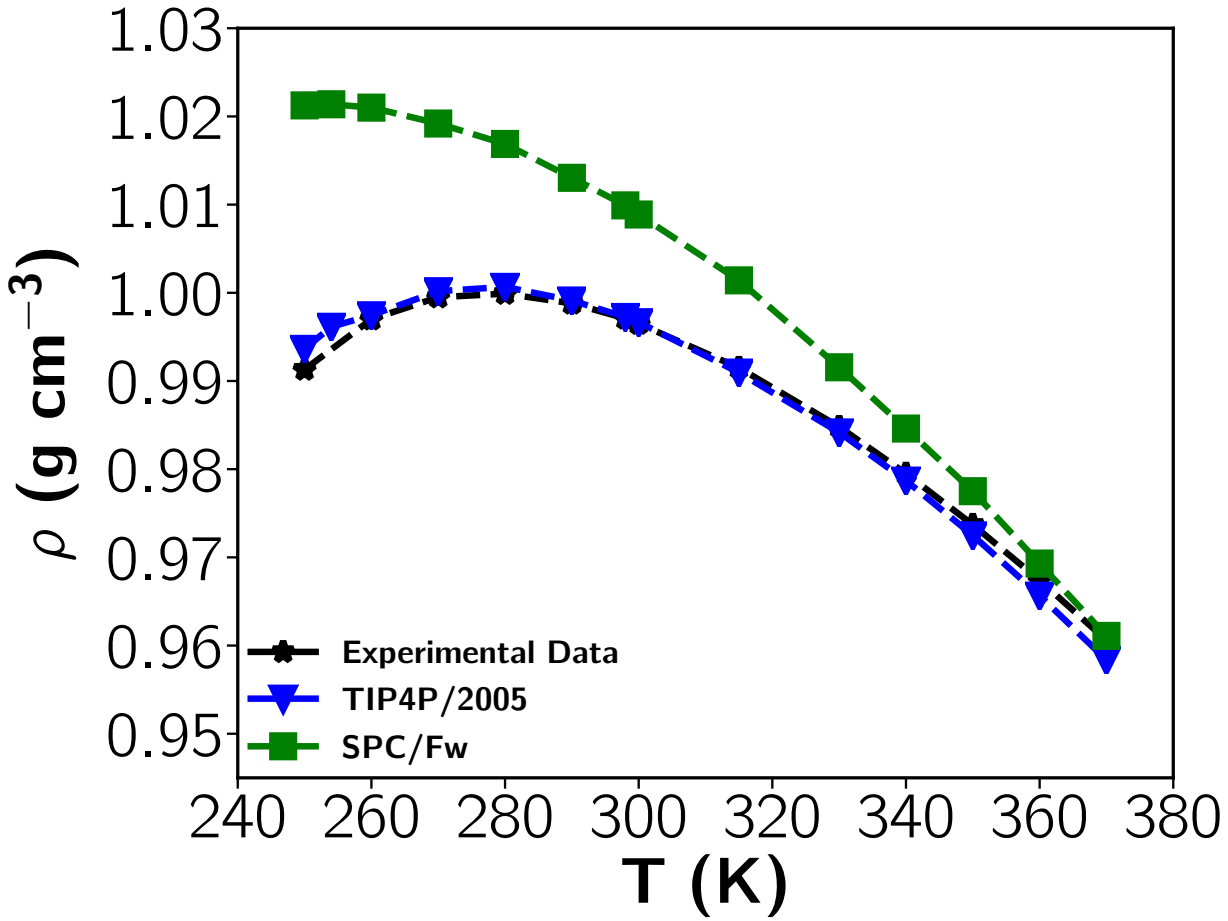

Figure 1: Density as a function of temperature comparing the results of TIP4P/2005 (triangles), and SPC/Fw (squares), and experimental data[62,63] (stars) at atmospheric pressure.

Another "volumetric" quantity is the thermal expansion coefficient. It was calculated through analytic differentiation of the polynomial fit of the densities. The calculated values for a range of temperatures are plotted in Figure 2. As expected, the TIP4P/2005 gives a good agreement with the data experiments along all the range of temperatures. The flexible model, however, gives the worst behavior when compared with the rigid atomistic model. The experimental expansion coefficient data illustrated in figure 2 were acquired through the analytic differentiation of the density experimental which was subsequently incorporated into the reference database.[62]

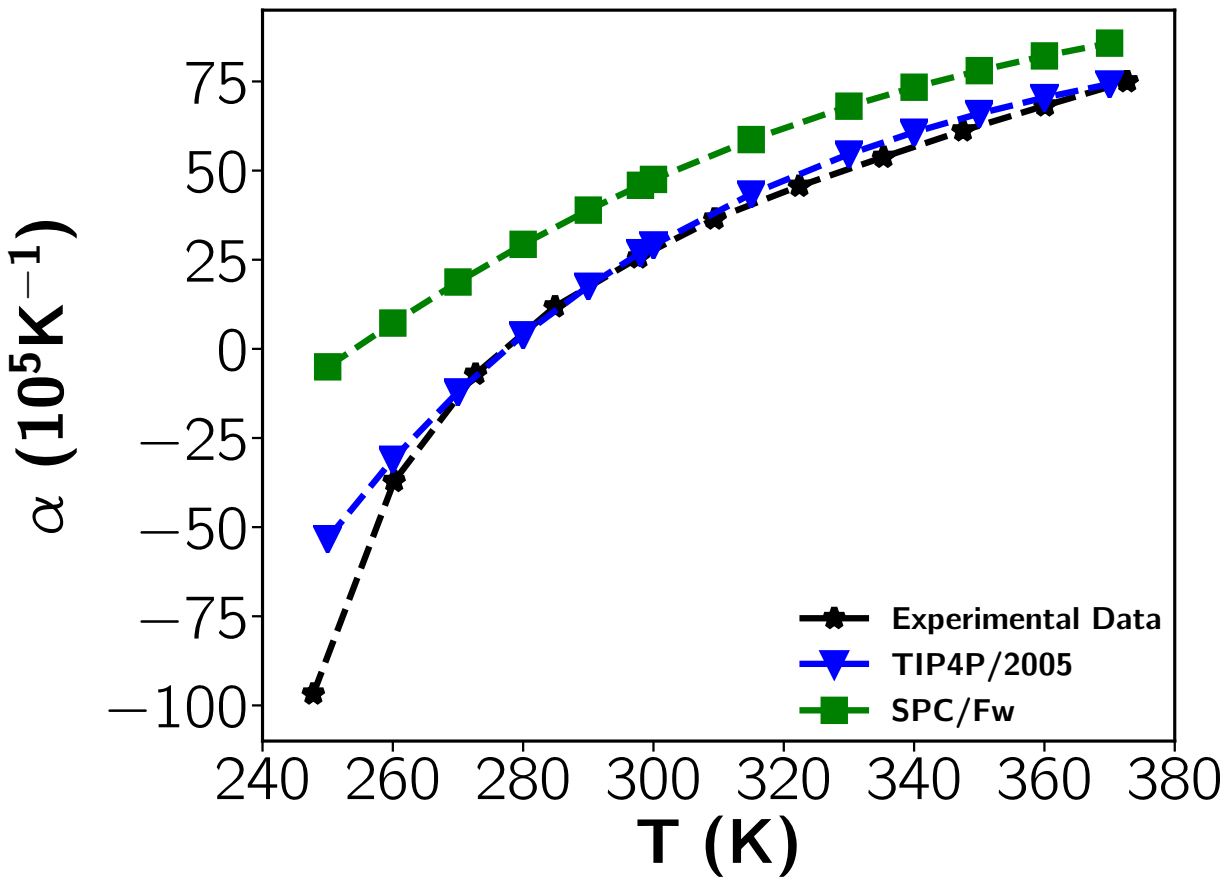

Figure 2: Thermal Expansion Coefficient comparing the results of TIP4P/2005 (triangles) and SPC/Fw (squares), and experimental data[62] (stars) at atmospheric pressure.

The density anomaly observed in liquid water is the result of a competition between the van der Waals and the hydrogen bond interactions between the molecules. As a result bonded and nonbonded clusters are formed. This is usually represented by two length scales interaction in effective models which are able to describe the effect.[54] Because the phenomenon can be explained in terms of sizes we called the volumetric effect and this is the reason that rigid models in which the bonds are present can represent it. In the flexible models, the competition between the two length scales becomes less important and as a result, they show a worst representation of the phenomena.

Self-Diffusion Coefficient, Shear Viscosity and Dielectric constant

Next, we analyze three properties in which the polar properties of water seem to be relevant.

First, in order to calculate the self-diffusion coefficient, the mean squared displacement (MSD) of oxygen atoms was obtained and plotted against time, as shown in Figure 3 for several temperatures, respectively. From the slope of the curves, the diffusion is calculated according to the Einstein equation,

$$6tD = \lim_{t\to\infty} \langle |\mathbf{r(t)} - \mathbf{r(0)}|^2 \rangle \tag{4}$$

Figure 3 shows the self-diffusion constant as a function of temperature. The models reproduce qualitatively the diffusion for with the increase of the temperature this property increases as well, as expected by the nature of intermolecular interactions. Both SPC/Fw and TIP4P/2005 models are in good agreement with the experimental curve. At 298 K, the SPC/Fw gives an error of 0.12%, followed by the rigid model with 17% with respect to the experimental value of $2.30 \times 10^{-9} m^2/s$.[64] The introduction of intramolecular degrees of freedom in the SPC/Fw model notably reduces the self-diffusion coefficients, obtaining satisfactory values when compared with the experimental data and with the TIP4P/2005 rigid model.

All the models exhibit a typical Arrhenius-like behavior expected for water. Furthermore, from the slope of the curves, the activation energy may be obtained, which gives a description of the hydrogen bonds dynamics. The TIP4P/2005 and SPC/Fw give energies of -18.2 kJ/mol and -17.0 kJ/mol, respectively, which agree with the experimental value of -17.8 kJ/mol.[65]

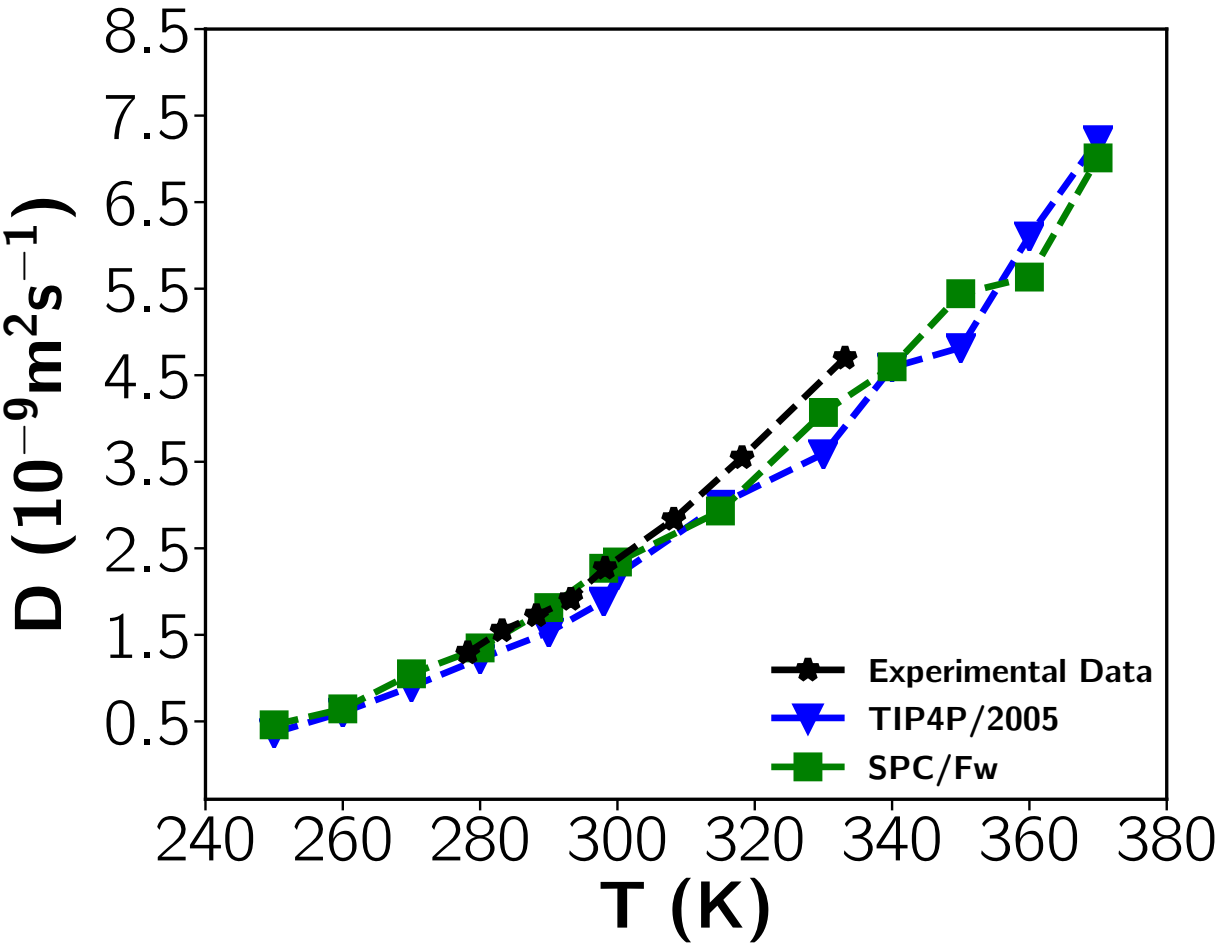

Figure 3: Water Self-Diffusion Coefficient as a function of temperature at 1 atm pressure comparing the results of TIP4P/2005 (triangles), SPC/Fw (squares), and experimental data[64] (stars). The experimental curve was omitted to preserve the graph scale and improve the visual comparison between the simulated results.[64]

Next, the viscosity was calculated with the Green-Kubo relation evaluated at equilibrium through a sufficiently long run in order to minimize the tail errors inherent to that method. The dependence of viscosity with temperature is plotted in Figure 4.

Both models reproduce, to a certain extent, the experimentally observed relation between viscosity and temperature, The TIP4P/2005 results converge well for higher temperatures (over 300 K), having an average deviation of 6.1% with respect to the experimental curve.[66] SPC/Fw gives a better description than TIP4P/2005 below 300 K, but its average deviation at all temperatures is large (49%) due to its overestimation above 300 K. The values sug-

gest that the flexible model gives a better performance than the rigid when compared with experimental results.

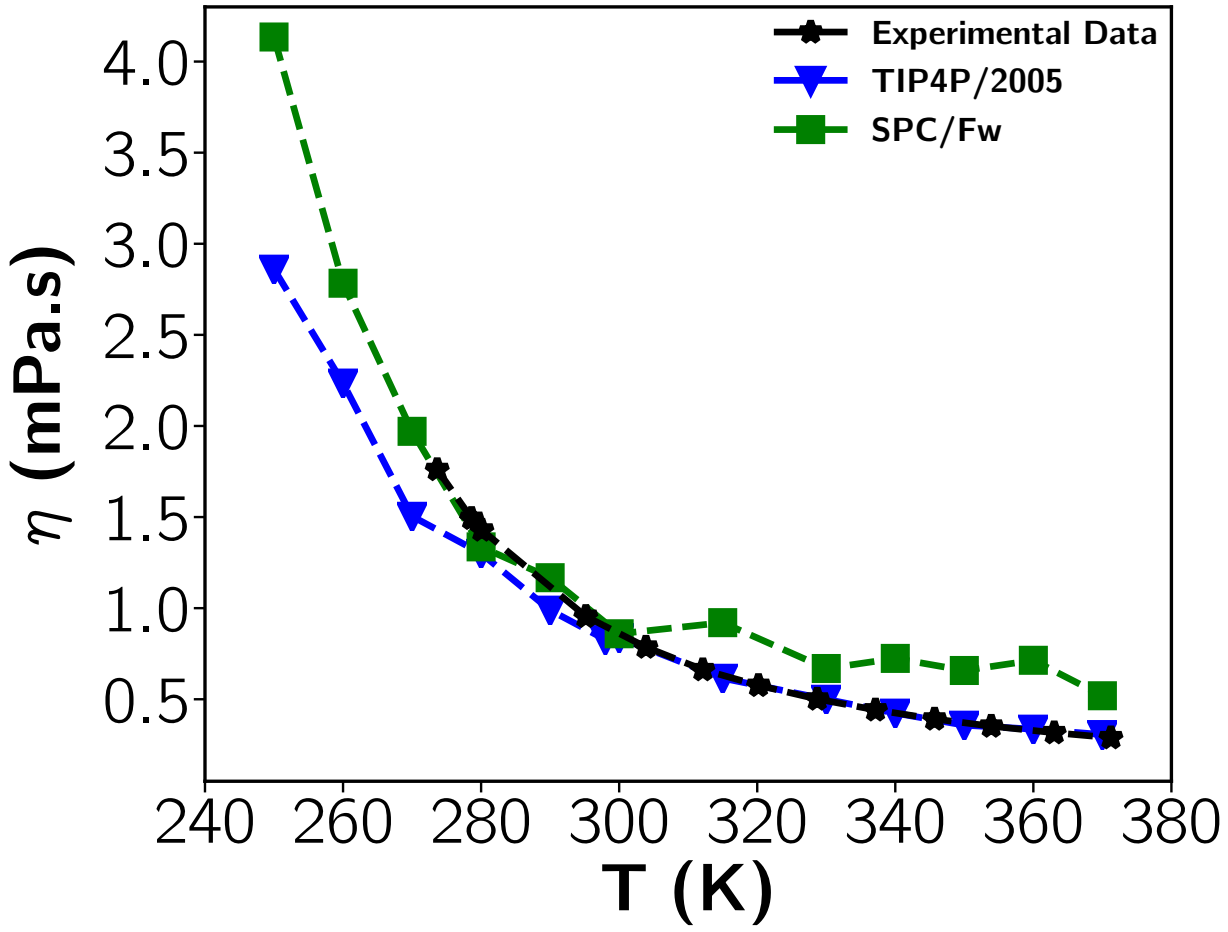

Figure 4: Comparing the Viscosity of water as a function of the temperature using TIP4P/2005 (triangles), SPC/Fw (squares), and experimental data[66](stars) at 1 atm pressure. Below 275 K, the experimental curve is extrapolated to compare with the results obtained for the model at the supercooled fluid region.

Next, we calculated the dielectric constant of bulk water. We employed the method proposed by Neumann, et al.[67] The static dielectric constant is computed from the fluctuations of the total dipole moment $\mathbf{M}$,

$$\epsilon_r = 1 + \frac{4\pi}{3K_B TV}(\langle \mathbf{M^2} \rangle - \langle \mathbf{M} \rangle^{\mathbf{2}}), \tag{5}$$

where K_B is the Boltzmann constant and T the absolute temperature. The dielectric constant is obtained for 40 ns simulations at constant density (1g/cm^3 and temperature or at constant temperature and pressure

Figure 5 shows the dielectric constant for water bulk using several temperatures for models TIP4P/2005 and SPC/Fw at density $1g/cm^3$ and $P = 1$ atm. The TIP4P/2005 model shows much lower values of dielectric constant when compared with the SPC/Fw model, other models for water[59] and experiments.[59,68] The results for SPC/Fw model follow the same trends as the experimental values[68] in all temperature ranges analyzed. The fact that the SPC/Fw gives a good estimate for the dielectric constant at room pressure and temperature is not surprising since the model was fitted to give this result. However, it does represent for a wide range of temperatures what suggests that the flexibility of the model allows for changes in the dipole moment with temperature.

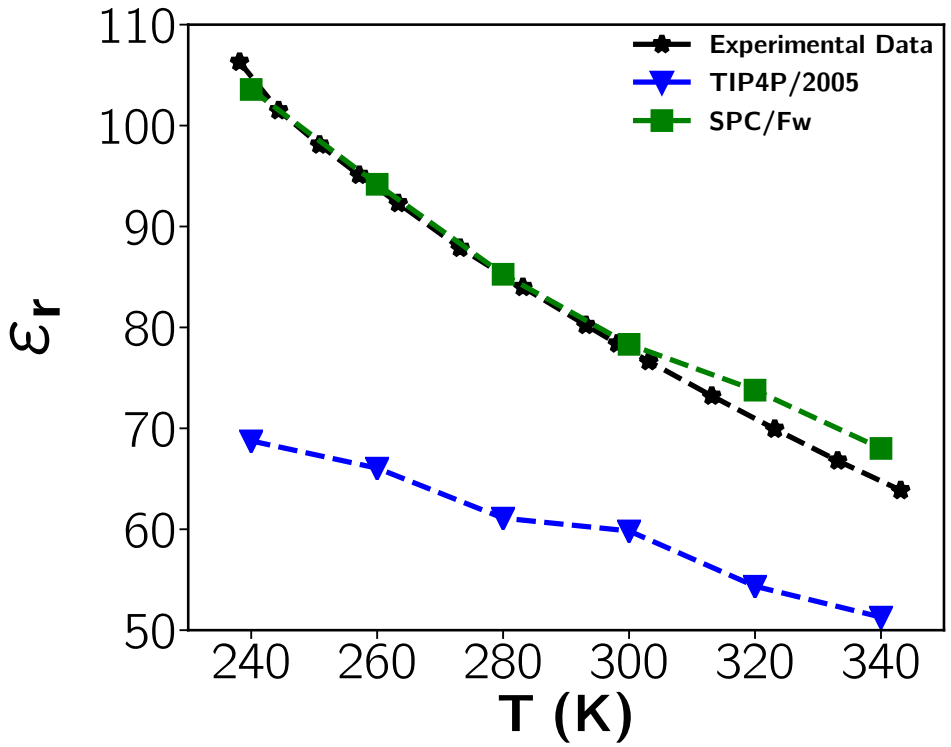

Figure 5: Calculated dielectric constant for water bulk using the TIP4P/2005 (triangles), SPC/Fw (squares) models, and experimental data[68](stars) at several temperatures at density $1g/cm^3$ and $P = 1$ atm.

Radial Distribution Function

Figures 6 (a)-(b) shows the radial distribution functions of the O-O pair for the different models, as well as their dependence on the temperature at atmospheric pressure and 1 g/cm^3. As expected, with increasing temperature, there is a significant loss of structure and ordering. The TIP4P/2005 model shows more structure with a higher first peak for low temperatures when compared with the SPC/Fw model but the distinction decreases as the temperature is increased.

To understand how the distinction of structure is compared with the actual water behavior, our results are compared with experimental results at 300 K. In figure 6 (c) a comparison is made, at a temperature of 300 K, between the models. The first peak of the graph, corresponding to the first solvation layer, is present in the two models at approximately the same height and the same distance. The coordination number associated with the first shell was calculated up to a distance of 0.487 nm, for TIP4P/2005 and SPC/Fw with 0.461 nm each. The SPC/Fw the high values of density are justified by the second solvation shell, as its corresponding coordination number (calculated up to 0.55 nm) is 23.09, slightly higher than TIP4P/2005 with 22.81 which is consistent with the TIP4P/2004 being more structures and with lower density.

Compared to the experimental G(r),[69] the models overestimate the height of the first peak, but the distance values to this peak are close to the experimental one, as well as the coordination numbers (experimental 4.67[69]).

Figure 6 (d) shows the radial distribution functions of the O-H pair T = 300 K for the different models. The models also produce an overestimation in the amplitude of the first peak of the O-H correlation compared with the experimental.[69–71] However, the SPC/FW model exhibits a first peak position that is approximately 0.18 nm,[69–71] in contrast to the TIP4P/2005 model, which positions it at 0.2 nm. For the second peak, the models are in agreement with the experiment is very good.

While the O-O pair distribution functions of the two models are quite similar, this is not

the case of the O-H pairs. The distinction between the two models is observed not only in all the peaks which indicates a distinct organization of the hydrogen bonds between the two models. The graph indicates that the oxygen-hydrogen network for the SPC/Fw is more compact at the first layer and less compact at the second layer which enhances mobility. When complying with the two models, the dipoles form a different network which might be the source for the different dielectric behavior of the two models.

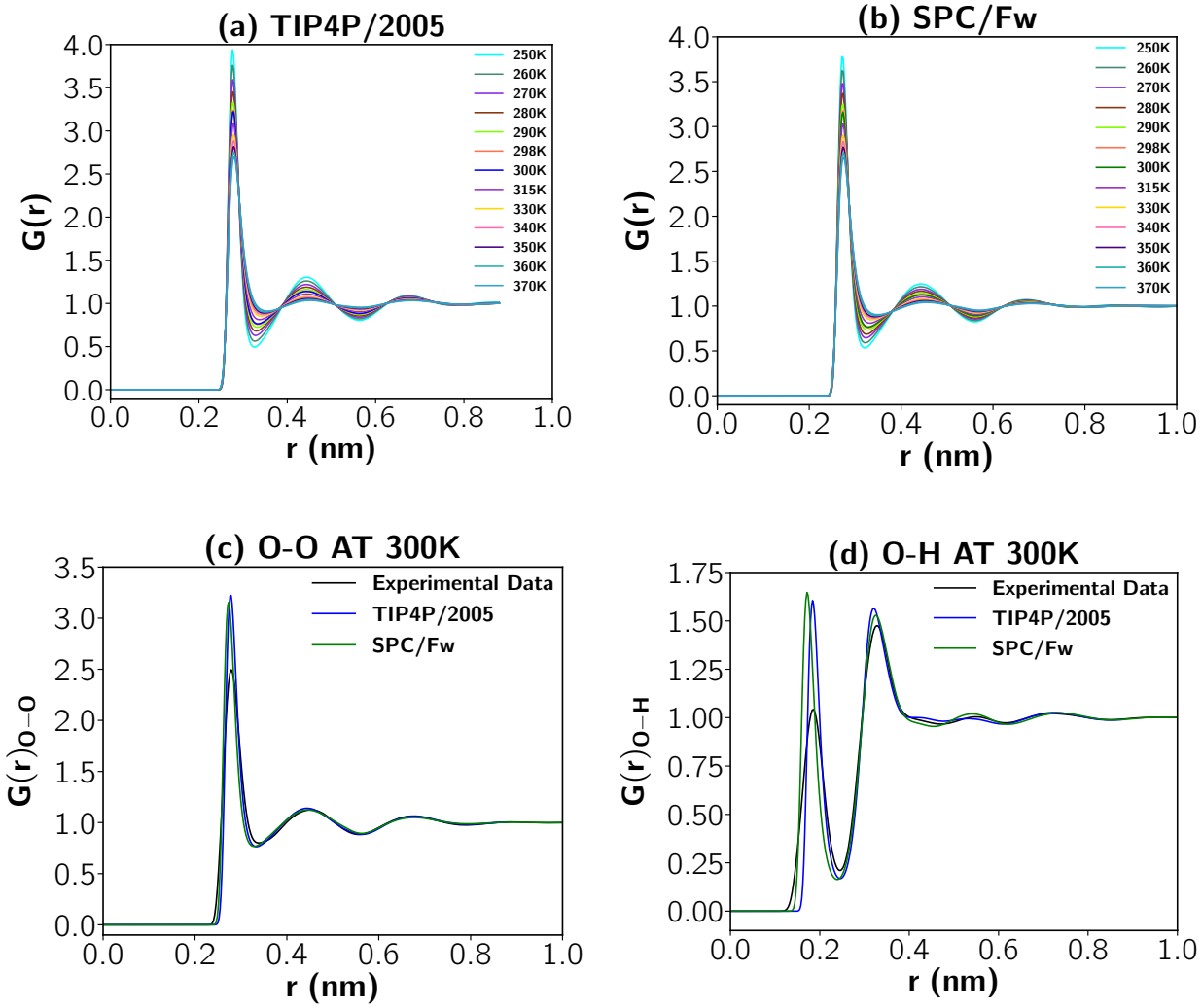

Figure 6: O-O pair distribution function at several temperatures (a) TIP4P/2005, (b) SPC/Fw, (c) O-O and (d) O-H pair distribution function at 300 K at atmospheric pressure and 1 g/cm^3.

Conclusions

We compared density, thermal expansion coefficient, self-diffusion coefficients, shear viscosity, radial distribution functions, and dielectric constant between the water models TIP4P/2005 and the flexible water model SPC/Fw at temperatures ranging from 250 K to 370 K.

Even though the TIP4P/2005 was parameterized to give the experimental density of water at 300 K, here we test how well the model performs for different temperatures and for other thermodynamic and dynamic properties. Similarly, the SPC/Fw was parameterized to give the value of the diffusion at room temperature we explore this model for thermodynamic properties and other temperatures.

The TIP4P/2005 model exhibited better behavior in thermodynamic properties compared to SPC/Fw. This is consistent with the fact that the TIP4P/2005 model was specifically fitted to yield good results in these properties, benefiting from the advantage of having more parameters to adjust than three-point models.

The SPC/Fw model offers a more accurate prediction for the dielectric constant at room pressure and various temperatures. This finding aligns with the notion that flexible models are advantageous for representing electrostatic-based properties.

The distinction between the two models becomes evident when examining the radial distribution function. While the O-O radial distribution function shows almost no difference which indicates that both models show the same number of water first neighbors, the O-H radial distribution function exhibits a clear distinction. For the SCP/Fw the oxygen of one molecule are closer to the hydrogens of the other, what indicates a lower number of hydrogen bonds. This disruption of the hydrogen bond network facilitates the mobility. In fact, the SPC/Fw model represents better the experimental results.

Our findings suggest that flexible models, even the simplest three-point case SPC/Fw, more effectively capture the long-range electrostatic structures. In contrast, rigid models, particularly the four-point model studied here, offer a more reliable description of thermodynamic properties.

Acknowledgement

This work is funded by the Brazilian scientific agency Conselho Nacional de Desenvolvimento Científico e Tecnológico (CNPq), the INCT Carbon Nanomaterials and INCT Materials Informatics. JVLV and EEM thank the science agency PIBIC-UFBA for financial support. Authors acknowledge the National Laboratory for Scientific Computing (LNCC/MCTI, Brazil) for providing HPC resources of the SDumont supercomputer, which have contributed to the research results reported within this paper. URL: `http://sdumont.lncc.br`.

References

(1) Lang, E. W.; Lüdemann, H.-D. Anomalies of liquid water. *Angewandte Chemie International Edition in English* **1982**, *21*, 315–329.

(2) Kell, G. S. Density, thermal expansivity, and compressibility of liquid water from 0. deg. to 150. deg.. Correlations and tables for atmospheric pressure and saturation reviewed and expressed on 1968 temperature scale. *Journal of Chemical and Engineering data* **1975**, *20*, 97–105.

(3) Angell, C.; Finch, E.; Bach, P. Spin–echo diffusion coefficients of water to 2380 bar and- 20° C. *The Journal of Chemical Physics* **1976**, *65*, 3063–3066.

(4) Netz, P. A.; Starr, F. W.; Stanley, H. E.; Barbosa, M. C. Static and dynamic properties of stretched water. *The Journal of chemical physics* **2001**, *115*, 344–348.

(5) Netz, P.; Starr, F.; Barbosa, M.; Stanley, H. E. Translational and rotational diffusion in stretched water. *Journal of Molecular Liquids* **2002**, *101*, 159–168.

(6) Majumder, M.; Chopra, N.; Andrews, R.; Hinds, B. J. Enhanced flow in carbon nanotubes. *Nature* **2005**, *438*, 44–44.

(7) Hummer, G.; Rasaiah, J. C.; Noworyta, J. P. Water conduction through the hydrophobic channel of a carbon nanotube. *Nature* **2001**, *414*, 188–190.

(8) Whitby, M.; Cagnon, L.; Thanou, M.; Quirke, N. Enhanced fluid flow through nanoscale carbon pipes. *Nano letters* **2008**, *8*, 2632–2637.

(9) Bordin, J. R.; Diehl, A.; Barbosa, M. C.; Levin, Y. Ion fluxes through nanopores and transmembrane channels. *Physical Review E* **2012**, *85*, 031914.

(10) Bordin, J. R.; Diehl, A.; Barbosa, M. C. Relation between flow enhancement factor and structure for core-softened fluids inside nanotubes. *The Journal of Physical Chemistry B* **2013**, *117*, 7047–7056.

(11) Bagchi, B. Anomalies of Water. *Water in Biological and Chemical Processes-From Structure and Dynamics to Function* **2013**, 13–26.

(12) Barbosa, M. C. Aprendendo com as esquisitices da água. *e-Boletim da Física* **2015**, *4*, 1–5.

(13) Holt, J. K.; Park, H. G.; Wang, Y.; Stadermann, M.; Artyukhin, A. B.; Grigoropoulos, C. P.; Noy, A.; Bakajin, O. Fast mass transport through sub-2-nanometer carbon nanotubes. *Science* **2006**, *312*, 1034–1037.

(14) Debenedetti, P. G.; Stanley, H. E. Supercooled and glassy water. *Physics Today* **2003**, *56*, 40–46.

(15) Ball, P. Water is an active matrix of life for cell and molecular biology. *Proceedings of the National Academy of Sciences* **2017**, *114*, 13327–13335.

(16) Franks, F. *Biophysics and biochemistry at low temperatures*; Cambridge University Press, 1985.

(17) Brini, E.; Fennell, C. J.; Fernandez-Serra, M.; Hribar-Lee, B.; Luksic, M.; Dill, K. A. How water's properties are encoded in its molecular structure and energies. *Chemical reviews* **2017**, *117*, 12385–12414.

(18) Boretti, A.; Rosa, L. Reassessing the projections of the world water development report. *NPJ Clean Water* **2019**, *2*, 15.

(19) UNESCO,, et al. *The United Nations World Water Development Report 2021: Valuing Water*; United Nations, 2021.

(20) Pointet, T. The United Nations World Water Development Report 2022 on Groundwater, a Synthesis. *LHB* **2022**, *108*, 2090867.

(21) Chavez, R. O.; Meseguer-Ruiz, O.; Olea, M.; Calderon-Seguel, M.; Yager, K.; Meneses, R. I.; Lastra, J. A.; Nunez-Hidalgo, I.; Sarricolea, P.; Serrano-Notivoli, R., et al. Andean peatlands at risk? Spatiotemporal patterns of extreme NDVI anomalies, water extraction and drought severity in a large-scale mining area of Atacama, northern Chile. *International Journal of Applied Earth Observation and Geoinformation* **2023**, *116*, 103138.

(22) Bridhikitti, A.; Ketuthong, A.; Prabamroong, T.; Li, R.; Li, J.; Liu, G. How do sustainable development-induced land use change and climate change affect water balance? A case study of the Mun River Basin, NE Thailand. *Water Resources Management* **2023**, *37*, 2737–2756.

(23) Chen, W.; Liu, S.; Zhao, S.; Zhu, Y.; Feng, S.; Wang, Z.; Wu, Y.; Xiao, J.; Yuan, W.; Yan, W., et al. Temporal dynamics of ecosystem, inherent, and underlying water use efficiencies of forests, grasslands, and croplands and their responses to climate change. *Carbon Balance and Management* **2023**, *18*, 1–14.

(24) van der Laan, E.; Nunes, J. P.; Dias, L. F.; Carvalho, S.; Santos, F. Assessing the climate change adaptability of sustainable land management practices regarding water

availability and quality: A case study in the Sorraia catchment, Portugal. *Science of The Total Environment* **2023**, 165438.

(25) Tripathy, K. P.; Mukherjee, S.; Mishra, A. K.; Mann, M. E.; Williams, A. P. Climate change will accelerate the high-end risk of compound drought and heatwave events. *Proceedings of the National Academy of Sciences* **2023**, *120*, e2219825120.

(26) Berendsen, H. J.; Postma, J. P.; van Gunsteren, W. F.; Hermans, J. *Interaction models for water in relation to protein hydration*; Springer Netherlands, 1981.

(27) Teleman, O.; Jönsson, B.; Engström, S. A molecular dynamics simulation of a water model with intramolecular degrees of freedom. *Molecular Physics* **1987**, *60*, 193–203.

(28) Abascal, J. L.; Vega, C. A general purpose model for the condensed phases of water: TIP4P/2005. *The Journal of Chemical Physics* **2005**, *123*, 234505.

(29) Kaminski, G. A.; Friesner, R. A.; Tirado-Rives, J.; Jorgensen, W. L. Evaluation and reparametrization of the OPLS-AA force field for proteins via comparison with accurate quantum chemical calculations on peptides. *The Journal of Physical Chemistry B* **2001**, *105*, 6474–6487.

(30) Horn, H. W.; Swope, W. C.; Pitera, J. W.; Madura, J. D.; Dick, T. J.; Hura, G. L.; Head-Gordon, T. Development of an improved four-site water model for biomolecular simulations: TIP4P-Ew. *The Journal of Chemical Physics* **2004**, *120*, 9665–9678.

(31) Jorgensen, W. L.; Chandrasekhar, J.; Madura, J. D.; Impey, R. W.; Klein, M. L. Comparison of simple potential functions for simulating liquid water. *The Journal of Chemical Physics* **1983**, *79*, 926–935.

(32) Mahoney, M. W.; Jorgensen, W. L. A five-site model for liquid water and the reproduction of the density anomaly by rigid, nonpolarizable potential functions. *The Journal of Chemical Physics* **2000**, *112*, 8910–8922.

(33) Vega, C.; Abascal, J. Relation between the melting temperature and the temperature of maximum density for the most common models of water. *The Journal of Chemical Physics* **2005**, *123*, 144504.

(34) López-Lemus, J.; Chapela, G. A.; Alejandre, J. Effect of flexibility on surface tension and coexisting densities of water. *The Journal of Chemical Physics* **2008**, *128*, 174703.

(35) Alejandre, J.; Chapela, G. A.; Bresme, F.; Hansen, J.-P. The short range anion-H interaction is the driving force for crystal formation of ions in water. *The Journal of Chemical Physics* **2009**, *130*, 174505.

(36) Zhang, L.; Wang, H.; Car, R.; Weinan, E. Phase diagram of a Deep potential water model. *Physical Review Letters* **2021**, *126*, 236001.

(37) Wallqvist, A.; Teleman, O. Properties of flexible water models. *Molecular Physics* **1991**, *74*, 515–533.

(38) Tocci, G.; Bilichenko, M.; Joly, L.; Iannuzzi, M. Ab initio nanofluidics: disentangling the role of the energy landscape and of density correlations on liquid/solid friction. *Nanoscale* **2020**, *12*, 10994–11000.

(39) Calegari Andrade, M. F.; Pham, T. A. Probing Confinement Effects on the Infrared Spectra of Water with Deep Potential Molecular Dynamics Simulations. *The Journal of Physical Chemistry Letters* **2023**, *14*, 5560–5566.

(40) Babin, V.; Leforestier, C.; Paesani, F. Development of a "first principles" water potential with flexible monomers: Dimer potential energy surface, VRT spectrum, and second virial coefficient. *Journal of Chemical Theory and Computation* **2013**, *9*, 5395–5403.

(41) Babin, V.; Medders, G. R.; Paesani, F. Development of a "first principles" water potential with flexible monomers. II: Trimer potential energy surface, third virial coefficient, and small clusters. *Journal of Chemical Theory and Computation* **2014**, *10*, 1599–1607.

(42) Medders, G. R.; Babin, V.; Paesani, F. Development of a "first-principles" water potential with flexible monomers. III. Liquid phase properties. *Journal of Chemical Theory and Computation* **2014**, *10*, 2906–2910.

(43) Das, A. K.; Urban, L.; Leven, I.; Loipersberger, M.; Aldossary, A.; Head-Gordon, M.; Head-Gordon, T. Development of an advanced force field for water using variational energy decomposition analysis. *Journal of Chemical Theory and Computation* **2019**, *15*, 5001–5013.

(44) Liu, C.; Piquemal, J.-P.; Ren, P. AMOEBA+ classical potential for modeling molecular interactions. *Journal of Chemical Theory and Computation* **2019**, *15*, 4122–4139.

(45) Liu, C.; Piquemal, J.-P.; Ren, P. Implementation of geometry-dependent charge flux into the polarizable AMOEBA+ potential. *The Journal of Physical Chemistry Letters* **2019**, *11*, 419–426.

(46) Rackers, J. A.; Silva, R. R.; Wang, Z.; Ponder, J. W. Polarizable water potential derived from a model electron density. *Journal of Chemical Theory and Computation* **2021**, *17*, 7056–7084.

(47) Lambros, E.; Paesani, F. How good are polarizable and flexible models for water: Insights from a many-body perspective. *The Journal of Chemical Physics* **2020**, *153*, 060901.

(48) Rieth, A. J.; Hunter, K. M.; Dincă, M.; Paesani, F. Hydrogen bonding structure of confined water templated by a metal-organic framework with open metal sites. *Nature Communications* **2019**, *10*, 4771.

(49) Wagner, J. C.; Hunter, K. M.; Paesani, F.; Xiong, W. Water capture mechanisms at zeolitic imidazolate framework interfaces. *Journal of the American Chemical Society* **2021**, *143*, 21189–21194.

(50) Medina, J.; Prosmiti, R.; Villarreal, P.; Delgado-Barrio, G.; Winter, G.; González, B.; Alemán, J.; Collado, C. Molecular dynamics simulations of rigid and flexible water models: Temperature dependence of viscosity. *Chemical Physics* **2011**, *388*, 9–18.

(51) Shvab, I.; Sadus, R. J. Atomistic water models: Aqueous thermodynamic properties from ambient to supercritical conditions. *Fluid Phase Equilibria* **2016**, *407*, 7–30, Aqueous Solutions.

(52) Mendonça, B. H.; de Moraes, E. E.; Batista, R. J.; de Oliveira, A. B.; Barbosa, M. C.; Chacham, H. Water diffusion in carbon nanotubes for rigid and flexible models. *The Journal of Physical Chemistry C* **2023**, *127*, 9769–9778.

(53) Wallqvist, A.; Teleman, O. Properties of flexible water models. *Molecular Physics* **1991**, *74*, 515–533.

(54) de Oliveira, A. B.; Netz, P. A.; Colla, T.; Barbosa, M. C. Thermodynamic and dynamic anomalies for a three-dimensional isotropic core-softened potential. *J. Chem. Phys.* **2006**, *124*, 84505.

(55) Wu, Y.; Tepper, H. L.; Voth, G. A. Flexible simple point-charge water model with improved liquid-state properties. *The Journal of Chemical Physics* **2006**, *124*, 024503.

(56) Mendonça, B. H. S.; de Moraes, E. E.; Kirch, A.; Batista, R. J. C.; de Oliveira, A. B.; Barbosa, M. C.; H., C. Flow through Deformed Carbon Nanotubes Predicted by Rigid and Flexible Water Models. *J. Phys. Chem. B* **2023**, *127*, 8634–8643.

(57) Vega, C.; Abascal, J. L.; Conde, M.; Aragones, J. What ice can teach us about water interactions: a critical comparison of the performance of different water models. *Faraday Discussions* **2009**, *141*, 251–276.

(58) Pi, H. L.; Aragones, J. L.; Vega, C.; Noya, E. G.; Abascal, J. L.; Gonzalez, M. A.; McBride, C. Anomalies in water as obtained from computer simulations of the

TIP4P/2005 model: density maxima, and density, isothermal compressibility and heat capacity minima. *Molecular Physics* **2009**, *107*, 365–374.

(59) Fuentes-Azcatl, R.; Barbosa, M. C. Thermodynamic and dynamic anomalous behavior in the TIP4P/ϵ water model. *Physica A: Statistical Mechanics and its Applications* **2016**, *444*, 86–94.

(60) Thompson, A. P.; Aktulga, H. M.; Berger, R.; Bolintineanu, D. S.; Brown, W. M.; Crozier, P. S.; in 't Veld, P. J.; Kohlmeyer, A.; Moore, S. G.; Nguyen, T. D.; Shan, R.; Stevens, M. J.; Tranchida, J.; Trott, C.; Plimpton, S. J. LAMMPS - a flexible simulation tool for particle-based materials modeling at the atomic, meso, and continuum scales. *Comp. Phys. Comm.* **2022**, *271*, 108171.

(61) Weldon, R.; Wang, F. Simulating a flexible water model as rigid: Best practices and lessons learned. *J. Chem. Phys.* **2023**, *158*, 134506.

(62) Kell, G. S. Density, thermal expansivity, and compressibility of liquid water from 0. deg. to 150. deg.. Correlations and tables for atmospheric pressure and saturation reviewed and expressed on 1968 temperature scale. *Journal of Chemical and Engineering Data* **1975**, *20*, 97–105.

(63) Wagner, W.; Pruß, A. The IAPWS formulation 1995 for the thermodynamic properties of ordinary water substance for general and scientific use. *Journal of physical and chemical reference data* **2002**, *31*, 387–535.

(64) Harris, K. R.; Woolf, L. A. Pressure and temperature dependence of the self diffusion coefficient of water and oxygen-18 water. *Journal of the Chemical Society, Faraday Transactions 1: Physical Chemistry in Condensed Phases* **1980**, *76*, 377–385.

(65) Tanaka, K. Measurements of self-diffusion coefficients of water in pure water and in aqueous electrolyte solutions. *J. Chem. Soc., Faraday Trans. 1* **1975**, *71*, 1127–1131.

(66) Viswanath, D. S.; Ghosh, T. K.; Prasad, D. H.; Dutt, N. V.; Rani, K. Y. *Viscosity of liquids: theory, estimation, experiment, and data*; Springer Science & Business Media, 2007.

(67) Neumann, M. Dipole moment fluctuation formulas in computer simulations of polar systems. *Molecular Physics* **1983**, *50*, 841–858.

(68) Fernandez, D. P.; Mulev, Y.; Goodwin, A.; Sengers, J. L. A database for the static dielectric constant of water and steam. *Journal of Physical and Chemical Reference Data* **1995**, *24*, 33–70.

(69) Soper, A. K. The radial distribution functions of water as derived from radiation total scattering experiments: Is there anything we can say for sure? *International Scholarly Research Notices* **2013**, *2013*, 1–67.

(70) Soper, A.; Phillips, M. A new determination of the structure of water at 25 C. *Chemical Physics* **1986**, *107*, 47–60.

(71) Soper, A.; Bruni, F.; Ricci, M. Site–site pair correlation functions of water from 25 to 400 C: Revised analysis of new and old diffraction data. *The Journal of chemical physics* **1997**, *106*, 247–254.